Collinear Resonance Ionization Spectroscopy of Neutron-Deficient Francium Isotopes

K. T. Flanagan,[1,*] K. M. Lynch,[1,2] J. Billowes,[1] M. L. Bissell,[3] I. Budinčević,[3] T. E. Cocolios,[1,2] R. P. de Groote,[3] S. De Schepper,[3] V. N. Fedosseev,[4] S. Franchoo,[5] R. F. Garcia Ruiz,[3] H. Heylen,[3] B. A. Marsh,[4] G. Neyens,[3] T. J. Procter,[1] R. E. Rossel,[4,6] S. Rothe,[4] I. Strashnov,[1] H. H. Stroke,[7] and K. D. A. Wendt[6]

[1]*School of Physics and Astronomy, The University of Manchester, Manchester M13 9PL, United Kingdom*
[2]*Physics Department, CERN, CH-1211 Geneva 23, Switzerland*
[3]*Instituut voor Kern- en Stralingsfysica, KU Leuven, B-3001 Leuven, Belgium*
[4]*Engineering Department, CERN, CH-1211 Geneva 23, Switzerland*
[5]*Institut de Physique Nucléaire d'Orsay, F-91406 Orsay, France*
[6]*Institut für Physik, Johannes Gutenberg-Universität Mainz, D-55128 Mainz, Germany*
[7]*Department of Physics, New York University, New York, New York 10003, USA*

(Received 13 August 2013; published 19 November 2013)

The magnetic moments and isotope shifts of the neutron-deficient francium isotopes $^{202\text{-}205}$Fr were measured at ISOLDE-CERN with use of collinear resonance ionization spectroscopy. A production-to-detection efficiency of 1% was measured for ^{202}Fr. The background from nonresonant and collisional ionization was maintained below one ion in 10^5 beam particles. Through a comparison of the measured charge radii with predictions from the spherical droplet model, it is concluded that the ground-state wave function remains spherical down to ^{205}Fr, with a departure observed in ^{203}Fr ($N = 116$).

DOI: 10.1103/PhysRevLett.111.212501 PACS numbers: 21.10.Ky, 21.10.Ft, 21.10.Hw, 27.80.+w

There are surprisingly few nuclear observables with which theorists can elucidate the nuclear force and interacting many-fermion problem. The laser spectroscopy technique reported here has measured two of these (the magnetic moment and mean-square charge radius) via the hyperfine interaction and isotope shift. This is achieved without introducing assumptions associated with any particular approach, making these measurements suitable for testing modern nuclear models. A variety of laser spectroscopy techniques now exists for studying short-lived radioactive isotopes, which broadly focus on either high resolution ($<$ 100 MHz linewidth) or high sensitivity ($<$ 1 atom/s) [1,2].

We report here the first measurements of ^{202,203,205}Fr, reaching 11 neutrons from the $N = 126$ shell closure. This has been made possible by a new highly sensitive, high-resolution technique of bunched collinear-beam resonance ionization spectroscopy (CRIS). The CRIS technique combines for the first time velocity bunching (provided by the collinear geometry [3,4]) and time bunching (to eliminate the duty loss of required pulsed laser systems). The high sensitivity is reached through a combination of the excellent overlap of laser and beam, and the high quantum efficiency of ion detectors. This new technique may be applied generally to all nuclides, but it is at the limits of nuclear stability that it will manifest its particular advantages.

The CRIS method was first proposed more than 30 years ago [5], and its sub-Doppler resolution was demonstrated by Schultz *et al.*, who measured the radioactive isotopes of ytterbium [6]. Since these isotopes were produced as a continuous beam, the duty cycle losses associated with pulsed lasers introduced a loss in efficiency by a factor of 30, which contributed to a low total experimental efficiency of 0.001%. With the installation of a gas-filled radio frequency quadrupole ion trap (ISCOOL) at ISOLDE, bunched ion beams that match the duty cycle of the pulsed lasers are now available [7]. This motivated the development of a dedicated experiment to exploit the CRIS technique applied to time-bunched beams. In the present case it allowed for the first time measurements of the neutron-deficient francium isotopes with half-lives as short as 300 ms and production rates below 100 atoms/s.

In our work the francium isotopes were produced through spallation reactions induced by 1.4 GeV protons, incident on a high temperature uranium carbide target (2000 °C) and surface ionized (ionization potential 4.07 eV [8]) with use of a tantalum ionizer tube. A schematic of the experiment is presented in Fig. 1. The beam was accelerated to 50 keV, mass separated, and subsequently cooled and trapped by the ISCOOL. The trapping time was synchronized with the repetition rate of the Nd:YAG laser (30 Hz) used to ionize the francium atoms. The bunched ion beam was transported from ISCOOL to the CRIS beam line and neutralized in-flight with use of a potassium vapor cell, which was grounded during this experiment [9]. A differential pumping region separates the neutralization cell from the laser-atom interaction region, which was kept at 8×10^{-9} mbar to reduce the process of nonresonant collisional ionization. The non-neutralized component of the beam was deflected within the differential pumping region. In the interaction region ($\sim$ 1.2 m long) the atom bunch was temporally and collinearly overlapped with two pulsed laser beams. The resonantly excited and ionized beam was then deflected to

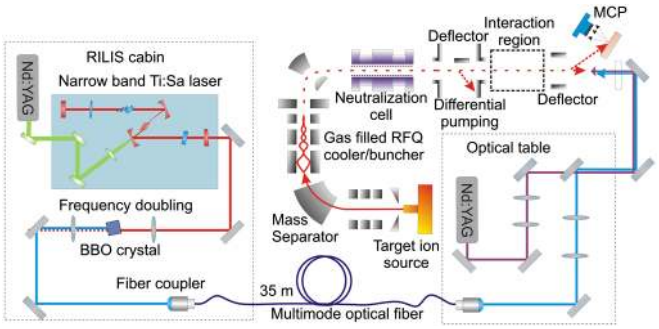

FIG. 1 (color online). Illustration of the CRIS experiment. The narrow-bandwidth Ti:sapphire laser was located in the RILIS laser cabin and fiber coupled to the CRIS experiment with 35 m of multimode fiber.

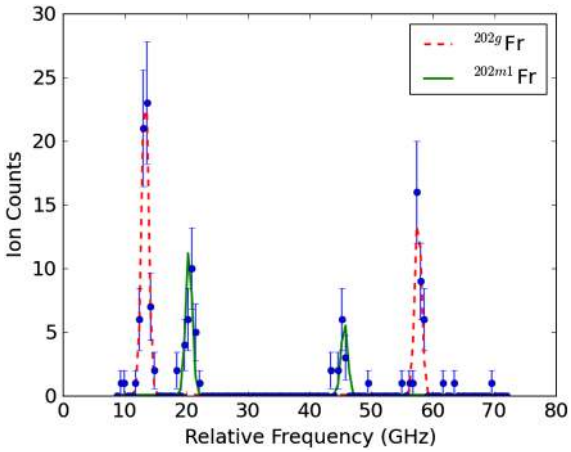

FIG. 2 (color online). Hyperfine spectra of the isomeric and ground state in ^{202}Fr. Fits for the $I^\pi = 10^-$ isomeric and $I^\pi = 3^+$ ground state are shown as solid and dashed lines, respectively.

either a microchannel plate detector [9] or decay spectroscopy station [10].

The phenomenon of shape coexistence in the lead region [11] has been studied recently through charge radii measurements of the neutron deficient lead [12] and polonium isotopes [13,14]. This work has shown a departure from a spherical charge distribution as it is predicted by the finite-range droplet model (FRDM). Self-consistent (beyond) mean field calculations conclude that towards the neutron midshell, the isotopes remain essentially spherical but with an increasingly collective contribution to the wave function: eventually in the lightest isotopes of polonium ($N < 104$) the wave functions shift towards an oblate deformed minimum [15]. A low energy two-particle two-hole ($2p$-$2h$) intruder $\pi(s_{1/2}^{-1})1/2^+$ state has been observed as an isomer [16–18]. This state has been reported to invert with the ground state in ^{199}Fr leading to an onset of ground-state deformation below $N = 113$ [19,20]. This makes the isotopes below ^{207}Fr represent a compelling case for laser spectroscopy. This Letter reports the application of CRIS with bunched beams to measure the magnetic moments and change in mean-square charge radii of the ground and long-lived isomeric states of $^{202-205}$Fr.

The isotopes were resonantly excited through the $7s^2S_{1/2} - 8p^2P_{3/2}$ transition (422.7 nm) and nonresonantly ionized by a 1064-nm photon. The laser light for the resonant step was produced by a narrow-bandwidth Ti:sapphire laser pumped by a 10-kHz Nd:YAG laser and constructed for in-source spectroscopy applications of the ISOLDE resonance ionization laser ion source (RILIS) [21]. The fundamental light from the Ti:sapphire laser was frequency doubled within the RILIS cabin and transported to an optical table next to the CRIS beam line using a multimode optical fiber (Fig. 1). The 422.7-nm laser was spatially overlapped with a 30-Hz Nd:YAG laser (Spectra-Physics Quanta-Ray). A trigger from the 10-kHz Nd:YAG pump laser was used to synchronize the Quanta-Ray laser, ISCOOL, and the data acquisition system.

During the experiment, the typical ion bunch width in the interaction region was 2–3 μs corresponding to a spatial length of 45–70 cm. A total experimental efficiency of 1% was determined for ^{202}Fr (Fig. 2), which was determined through a comparison of the resonant ion rate to the measured yield of 100 atoms/s [22]. This represents a factor of 1000 better than in the earlier CRIS measurements on ytterbium. The efficiency includes losses associated with beam transport, neutralization, ionization and detection, and was measured with 10 mW average power for the 422-nm laser and 15 mJ for the 1064-nm radiation, measured after the interaction region. The very few background events observed in Fig. 2 are associated with the nonresonant collisional ionization of the isobar ^{202}Tl, which has a production yield of $\sim 10^4$ atoms/μC. The nonresonant ionization efficiency was determined to be less than 1:10^5. The hyperfine structures associated with the ground and isomeric states in ^{202}Fr were identified with the decay spectroscopy station. The spectra were recorded by scanning the frequency of the Ti:sapphire laser in either 10 seconds or in proton-supercycle steps (typically 45–60 s). The ion signal detected by the microchannel plate was digitized by a 2.5-GHz oscilloscope (LeCroy WavePro) and recorded.

Reference scans of ^{221}Fr were taken at regular intervals during the experiment to account for any drifts in the measured frequency. From these reference scans the A factor of ^{221}Fr was measured to be $A(^2S_{1/2}) = +6200(30)$ MHz, which agrees closely with the literature value $+6204.6(8)$ MHz [23]. The measured scatter of the reference isotope A factor was used to determine the minimum error of the new measurements. The spectra for ^{203,205}Fr and reference ^{207}Fr are shown in Fig. 3.

The magnetic moments were evaluated from the measured $A(^2S_{1/2})$ values and calibrated using the spin and absolute magnetic moment measured in ^{210}Fr: $A(^2S_{1/2}) = +7195.1(4)$ MHz, $I^\pi = 6^+$, and $\mu = +4.38(5)\mu_N$ [23,24]. The A factors and magnetic moments were determined using assigned spins based on previous alpha-decay

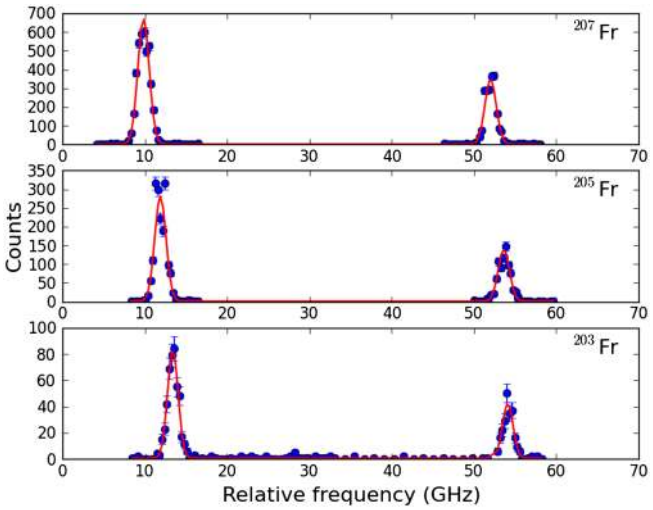

FIG. 3 (color online). Hyperfine spectra of the ground states in ^{203,205,207}Fr.

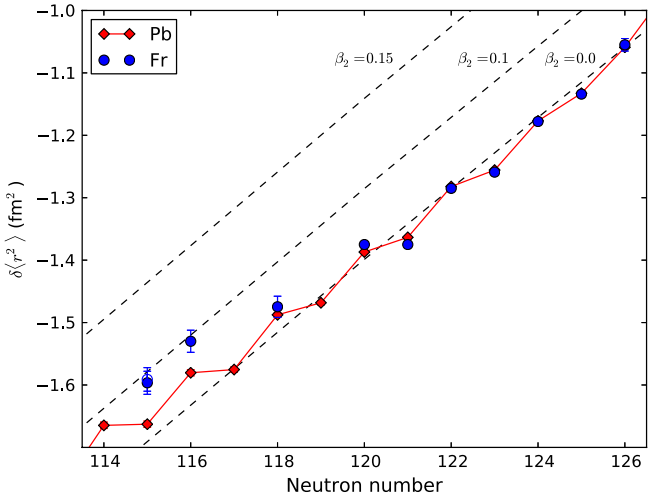

FIG. 4 (color online). $\delta\langle r^2\rangle$ of the neutron-deficient francium isotopes. The $I^\pi = 10^-$ isomeric state in ^{202}Fr is shown as an open symbol. Data for $^{207-213}$Fr ($N = 120$–126) are taken from [23]. The data are compared to the trend of $\delta\langle r^2\rangle$ in the lead isotopes [30]. Iso-deformation lines for constant $\beta_2 = 0$, 0.1, and 0.15 are shown as dashed lines [31,32]. The experimental data were fixed using $\beta_2 = 0$ for $N = 126$ according to the prediction by FRDM [35].

measurements of the isotopes and isomers, since direct spin measurement was not possible with the current experimental resolution [16,17,25]. The results are summarized in Table I.

The charge radii were extracted from measured isotope shifts using the King plot method and are presented in Table I [2,26]. Measurements of the isotope shifts $\delta\nu^{207,221}$ and $\delta\nu^{211,221}$ for the $7s^2S_{1/2} - 8p^2P_{3/2}$ transitions were combined with literature values for ^{212,213,220}Fr [27] and compared to the charge radii determined from the isotope shifts of the $7s^2S_{1/2} - 7p^2P_{3/2}$ transition (718.2 nm). Previous theoretical studies of the isotope shifts of the 718.2-nm line have determined the atomic factors for the field shift (F) and mass shift (M) with an estimated uncertainty of 1%–2% [28,29]. Using the calculations and the isotope shifts for both the 718.2-nm and 422.7-nm lines, a field shift of $F_{422} = -20.67(21)$ GHz/fm^2 and mass factor of $M_{422} = +750(330)$ GHz amu were determined. The uncertainty associated with F_{422} and M_{422} introduces a systematic scaling error which is up to a factor of 2 larger than the observed experimental errors (Table I).

The extracted $\delta\langle r^2\rangle$ for $^{202-213}$Fr are presented in Fig. 4 and compared to the $\delta\langle r^2\rangle$ of the lead isotope chain [30] and the iso-deformation lines for $\beta_2 = 0$, 0.1, and 0.15, derived using the second parametrization of the FRDM [31,32]. There is a remarkably close correlation between the odd-even staggering trend in the lead and francium isotope chains between $N = 118$ and $N = 126$. A departure from the trend observed is seen at $N = 116$, suggesting an earlier onset of deformation in the neutron-deficient francium isotopes than in the polonium or lead chains, where this happens below $N = 114$ [12,14]. The band structure built onto the ground state of ^{203,205}Fr suggests that while these isotopes have an increased collectivity, they remain spherical [17,18]. The magnetic moments of ^{203,205}Fr closely match the steadily decreasing trend from $\mu = +4.02(8)\mu_N$ at $N = 126$ [23] to $\mu = +3.73(4)\mu_N$ at $N = 116$, suggesting that the ground state is still dominated by a spherical $\pi(h^5_{9/2})$ configuration. An almost spherical system is also supported by the ground-state intrinsic quadrupole moment of ^{205}Fr, $Q_0 = -64.4(7)e$ fm^2, which

TABLE I. Summary of the measured hyperfine parameters, isotope shifts, and nuclear observables. The two errors shown for the extracted $\delta\langle r^2\rangle$ data correspond to the experimental errors and errors associated with the evaluated F_{422} and M_{422} atomic factors, respectively. A factors are based on assigned spins (see text for details).

Mass	I	$A(^2S_{1/2})$ (MHz)	$\delta\nu^{A,221}$ (MHz)	μ (μ_N)	$\delta\langle r^2\rangle^{A,221}$ (fm^2)
202	(3^+)	+12 800(50)	32 680(100)	+3.90(5)	−1.596(8)(16)
202	(10^-)	+2 300(30)	32 570(130)	+2.34(4)	−1.591(9)(16)
203	$(9/2^-)$	+8 180(30)	31 320(100)	+3.73(4)	−1.530(8)(16)
205	$9/2^-$	+8 400(30)	30 210(100)	+3.83(5)	−1.475(7)(15)

corresponds to a $\beta_2 = -0.0204(2)$ [33]. Using the FRDM to interpret the charge radii, a rms value for $\beta_2 = 0.06$ is calculated from $\delta\langle r^2\rangle^{118,126}$. While both analyses show that β_2 is much smaller than what is recognized as a deformed nucleus, the magnetic moments indicate that these nuclei are in a transition region between simple single-particle and collective behavior [33]. To understand this transition region will require beyond mean-field calculations or shell-model calculations with an extended basis that considers excitation across $Z = 82$. The measured magnetic moments reported here indicate that the departure of $\delta\langle r^2\rangle$ from the lead trend at N=116 is almost purely dynamic in origin and associated with zero-point fluctuations about the minimum of the potential well. This is supported by the fact that the rms β_2 deduced from $\delta\langle r^2\rangle^{118,126}$ is three times larger than the static β_2 deduced from the measured quadrupole moments [33].

This Letter reports the first laser spectroscopy measurements with the new CRIS experimental facility at ISOLDE, CERN. Magnetic moments and charge radii of the ground states and one isomer in the neutron-deficient francium isotopes $^{202-205}$Fr have been measured. The CRIS technique used in this work has demonstrated a total experimental efficiency of 1%. The background from nonresonant and collisional ionization has been maintained below one ion in 10^5 beam particles by maintaining a pressure in the interaction region of 8×10^{-9} mbar. This combination of high detection efficiency and ultra-low background has made it possible to study isotopes of francium produced at a rate that is 2 orders of magnitude lower than required with fluorescence based techniques [33]. The measured charge radii demonstrate early departure from spherical FRDM predictions and the parallel trend observed in the lead isotopes at $N = 116$. Based on systematics of the heavier isotopes in the region, this is interpreted as an increasingly collective yet spherical ground-state wave function. Measurement of the spectroscopic quadrupole moments down to ^{202}Fr would assist in understanding the evolution of the nuclear wave function in this region. Such measurements using high-resolution lasers are in preparation. A comparison of the results reported here with beyond mean field calculations of the type already performed on lead and polonium would further help understand the collective contributions to the wave function with increasing neutron holes [34].

This work has been supported by the Science and Technology Facilities Council consolidated Grant No. ST/F012071/1 and continuation Grant No. ST/J000159/1, the EU Seventh Framework through ENSAR(506065), the BriX Research Program No. P7/12, FWO-Vlaanderen (Belgium). K. T. Flanagan was supported by STFC Advanced Fellowship Scheme Grant No. ST/F012071/1. We would like to thank the ISOLDE technical group for their support and assistance. We acknowledge the financial aid from the Ed Schneiderman Fund at NYU.

*kieran.flanagan-2@manchester.ac.uk

[1] K. Blaum, J. Dilling, and W. Nörtershäuser, Phys. Scr. **T152**, 014017 (2013).
[2] B. Cheal and K. T. Flanagan, J. Phys. G **37**, 113101 (2010).
[3] W. H. Wing, G. A. Ruff, W. E. Lamb, and J. J. Spezeski, Phys. Rev. Lett. **36**, 1488 (1976).
[4] S. L. Kaufman, Opt. Commun. **17**, 309 (1976).
[5] Y. A. Kudriavtsev and V. S. Letokhov, Appl. Phys. B **29**, 219 (1982).
[6] C. Schulz *et al.*, J. Phys. B **24**, 4831 (1991).
[7] E. Mané *et al.*, Eur. Phys. J. A **42**, 503 (2009).
[8] S. V. Andreev, V. S. Letokhov, and V. I. Mishin, Phys. Rev. Lett. **59**, 1274 (1987).
[9] T. J. Procter *et al.*, J. Phys. Conf. Ser. **381**, 012070 (2012).
[10] M. M. Rajabali *et al.*, Nucl. Instrum. Methods Phys. Res., Sect. A **707**, 35 (2013).
[11] K. Heyde and J. L. Wood, Rev. Mod. Phys. **83**, 1467 (2011).
[12] H. DeWitte *et al.*, Phys. Rev. Lett. **98**, 112502 (2007).
[13] T. E. Cocolios *et al.*, Phys. Rev. Lett. **106**, 052503 (2011).
[14] M. D. Seliverstov *et al.*, Phys. Lett. B **719**, 362 (2013).
[15] T. Grahn *et al.*, Nucl. Phys. **A801**, 83 (2008).
[16] J. Uusitalo *et al.*, Phys. Rev. C **71**, 024306 (2005).
[17] U. Jakobsson *et al.*, Phys. Rev. C **87**, 054320 (2013).
[18] U. Jakobsson *et al.*, Phys. Rev. C **85**, 014309 (2012).
[19] J. Uusitalo *et al.*, Phys. Rev. C **87**, 064304 (2013).
[20] Z. Kalaninová *et al.*, Phys. Rev. C **87**, 044335 (2013).
[21] S. Rothe *et al.*, Nucl. Instrum. Methods Phys. Res., Sect. B, doi:10.1016/j.nimb.2013.08.058 (2013).
[22] A. Andreyev (private communication).
[23] A. Coc *et al.*, Phys. Lett. **163B**, 66 (1985).
[24] E. Gomez, S. Aubin, L. A. Orozco, G. D. Sprouse, E. Iskrenova-Tchoukova, and M. S. Safronova, Phys. Rev. Lett. **100**, 172502 (2008).
[25] M. Huyse, P. Decrock, P. Dendooven, G. Reusen, P. Van Duppen, and J. Wauters, Phys. Rev. C **46**, 1209 (1992).
[26] B. Cheal, T. E. Cocolios, and S. Fritzsche, Phys. Rev. A **86**, 042501 (2012).
[27] H. T. Duong *et al.*, Europhys. Lett. **3**, 175 (1987).
[28] V. A. Dzuba, W. R. Johnson, and M. S. Safronova, Phys. Rev. A **72**, 022503 (2005).
[29] A. M. Mårtensson-Pendrill, Mol. Phys. **98**, 1201 (2000).
[30] M. Anselment, W. Faubel, S. Göring, A. Hanser, G. Meisel, H. Rebel, and G. Schatz, Nucl. Phys. **A451**, 471 (1986).
[31] W. D. Myers and K.-H. Schmidt, Nucl. Phys. **A410**, 61 (1983).
[32] D. Berdichevsky and F. Tondeur, Z. Phys. A **322**, 141 (1985).
[33] A. Voss, M. R. Pearson, J. Billowes, F. Buchinger, B. Cheal, J. E. Crawford, A. A. Kwiatkowski, C. D. Philip Levy, and O. Shelbaya, Phys. Rev. Lett. **111**, 122501 (2013).
[34] M. Bender, G. F. Bertsch, and P.-H. Heenen, Phys. Rev. C **73**, 034322 (2006).
[35] P. Möller, J. R. Nix, W. D. Myers, and W. J. Swiatecki, At. Data Nucl. Data Tables **59**, 185 (1995).